Constitutive Laws for Jointed Rock Mass

N.K. Samadhiya

Department of Civil Engineering
Indian Institute of Technology
Roorkee – 247 667 (India)
Phone : +91-01332-285467(O); 285052 (R)
Fax : 01332 - 273560
Email : nksamfce@iitr.ernet.in

ABSTRACT

The rock masses essentially consist of two constituents: intact rock and discontinuities. The presence of these natural discontinuities such as joints and bedding planes in rock masses can exert a significant influence on the response of rock masses in both surface and underground excavations. The existence of one or several sets of discontinuities in rock mass creates anisotropy in its response to the applied stress field. The discontinuities may be oriented arbitrarily in any direction. Before any of these influences may be evaluated for a given rock engineering project, it is necessary that the discontinuities in the rock mass be properly characterized and their properties established. Three approaches can be followed to account for the effect of joints on rock mass strength and deformability. The first approach consists of empirically reducing the strength and modulus of a rock mass from those measured on intact rock samples in a laboratory. In the second approach, an intact rock is modelled using solid isotropic elements, whereas the joints are modelled explicitly using special joint elements to introduce the complex response of joints to normal and shear stresses. The third approach, which has been described in the present paper, is to treat a jointed rock mass as an equivalent anisotropic continuum. The approach aims to capture the overall behaviour of the rock mass based on the constitutive characteristics of intact rock and rock joints including their orientation, spacing, roughness (waviness), number of joint sets, block size and normal and shear stiffness etc. The constitutive relationships for jointed rock mass have been derived and applied to analyse an underground tunnel using a software package developed for the purpose.

***Keywords*: **Discontinuities; Rock masses; Underground excavations; Strength; Deformability; Strain energy; Equivalent anisotropic continuum.

1. INTRODUCTION

The presence of joints in rock mass has a pronounced effect on the mechanical behavior of rock mass. To accommodate these effects, two approaches were suggested for modeling the jointed rock masses. The joints may be included explicitly in mathematical relations or to be implicitly represented in constitutive relations. Evaluation of parameters associated with constitutive laws of intact rock and rock joints via large-scale in-situ tests is difficult and is usually very expensive. Under such circumstances, studies related to rock masses are extremely important from the standpoint of both research and practice. Duncan and Goodman (1968) replaced regularly jointed rock mass by an equivalent orthotropic continuum. The average strain energy concept was adopted by many research workers (Hill, 1963 and Singh, 1973) for deriving the constitutive equations of rock mass with orthogonal sets of discontinuous joints intersecting an isotropic rock material. Gerrard (1982) pointed out that the total strain, total compliance, and total stiffness of jointed rock mass may be obtained from the addition of these components for the rock material and each of the joint sets in global coordinates. Fossum (1985) treated the rock joint as a one-dimensional continuum characterized by joint shear and normal stiffnesses while the intact rock is modeled as a three-dimensional continuum with isotropic elastic properties. The rock mass system used was also studied earlier by Amadei and Goodman (1981) in which the effective modulus was found to depend on joint spacing, elastic properties of joint and elastic properties of the intact rock. Alehossein and Carter (1990) developed a set of anisotropic elasto-plastic constitutive relations to define the overall behavior of the rock mass. Indraratna (1990) examined the effect of the arrangement of joints on the overall response of jointed rock mass based on linear joints simulated with a pair of hardened plastered surface prepared by using gypsum, cement, and water. Yamabe et al. (1990) derived an elastic compliance tensor of jointed rock masses by treating each crack as a set of parallel plates connected by two springs. A multi laminate model for jointed rock mass was proposed by Pande (1993) based on an equivalent material approach. Cai and Horii (1993) developed a constitutive model for jointed rock masses, which reflects the size, density, orientation and connectivity of joints as well as their mechanical properties. Wang and Garga (1993) proposed a block-spring model to analyze the stress and deformation behavior of the jointed rock mass including large displacements. Amadei (1996) recommended the use of nonlinear elasticity or more complex constitutive behavior if the permanent deformation occurs, as the linear elasticity may be of a limited value while describing the deformability of anisotropic rock. However, the linear anisotropic elasticity analysis can yield reasonable results if the properties of rock are similar to in-situ condition in the range of stress under consideration. The anisotropy decreases with an increase in confinement. Prat et al. (1997) suggested an approach for modeling the anisotropy based on the use of micro-mechanical properties to obtain a macroscopic stress-strain relationship. Sitharam and Latha (2002) improved the capability of equivalent continuum approach and the joint factor model for the stress analysis of an excavation in jointed rock. A two scale concept was proposed by Ku et al. (2004) for modeling the behavior of jointed rock masses using a combined equivalent continuum approach and discrete approach.

This paper presents the constitutive relationships for jointed rock mass. The approach considers the jointed rock mass as an equivalent anisotropic continuum. An underground tunnel problem of Wittke (1990) has been analyzed. The results have compared well.

2. DERIVATION OF CONSTITUTIVE LAWS

2.1 Resolution of Stresses along a Joint Plane

Figure 1a shows a joint plane in global reference co-ordinates system. In global X,Y,Z co-ordinate system of axes, the Z-axis is taken in vertical direction and α_x represents the trend of X-axis with respect to global North and measured in the clock-wise direction. The dip direction and the dip of the joint plane (of j^{th} joint set) are α_j and ω_j respectively. Stresses on the inclined joint plane can be obtained by resolving the stresses in two stages. Firstly, the stresses are resolved along X′,Y′,Z′ axes where Z′-axis is vertical while the Y′ axis is parallel to the strike of the joint plane and X′ represents the direction of horizontal trace of the line of dip. In the following derivation, anti-clockwise angles between axes are taken as positive. Figure 1a shows the rotation of X′,Y′,Z′ axes with respect to the reference X,Y,Z axes and it has been defined by the following direction cosines:

$$\begin{aligned} l_1 &= \cos(\alpha_x - \alpha_j), & l_2 &= \sin(\alpha_j - \alpha_x), & l_3 &= 0 \\ m_1 &= \sin(\alpha_x - \alpha_j), & m_2 &= \cos(\alpha_j - \alpha_x), & m_3 &= 0 \\ n_1 &= 0, & n_2 &= 0, & n_3 &= 1 \end{aligned} \tag{1}$$

The rotation from X,Y,Z axes to X′,Y′,Z′ axes can be performed through the transformation matrix, [T_j'] which represented as follows:

$$\left[T_j'\right] = \begin{bmatrix} l_1^2 & m_1^2 & n_1^2 & 2\,l_1\,m_1 & 2\,m_1\,n_1 & 2\,n_1\,l_1 \\ l_2^2 & m_2^2 & n_2^2 & 2\,l_2\,m_2 & 2\,m_2\,n_2 & 2\,n_2\,l_2 \\ l_3^2 & m_3^2 & n_3^2 & 2\,l_3\,m_3 & 2\,m_3\,n_3 & 2\,n_3\,l_3 \\ l_1\,l_2 & m_1\,m_2 & n_1\,n_2 & (m_1\,l_2 + l_1\,m_2) & (n_1\,m_2 + m_1\,n_2) & (n_1\,l_2 + l_2\,n_1) \\ l_2\,l_3 & m_2\,m_3 & n_2\,n_3 & (m_2\,l_3 + l_2\,m_3) & (n_2\,m_3 + m_2\,n_3) & (n_2\,l_3 + l_2\,n_3) \\ l_1\,l_3 & m_1\,m_3 & n_1\,n_3 & (m_1\,l_3 + l_1\,m_3) & (n_1\,m_3 + m_1\,n_3) & (n_1\,l_3 + l_1\,n_3) \end{bmatrix} \tag{2}$$

The first transformation matrix, [T_j'] can be re-written after substituting the direction cosines of Eq. 1 into Eq. 2 as,

$$\left[T_j'\right] = \begin{bmatrix} \cos^2\lambda & \sin^2\lambda & 0 & \sin 2\lambda & 0 & 0 \\ \sin^2\lambda & \cos^2\lambda & 0 & -\sin 2\lambda & 0 & 0 \\ 0 & 0 & 1 & 1 & 0 & 0 \\ -\frac{1}{2}\sin 2\lambda & \frac{1}{2}\sin 2\lambda & 0 & \cos 2\lambda & 0 & 0 \\ 0 & 0 & 0 & 0 & \cos\lambda & -\sin\lambda \\ 0 & 0 & 0 & 0 & \sin\lambda & \cos\lambda \end{bmatrix} \tag{3}$$

where, $\lambda = (\alpha_x - \alpha_j)$ (4)

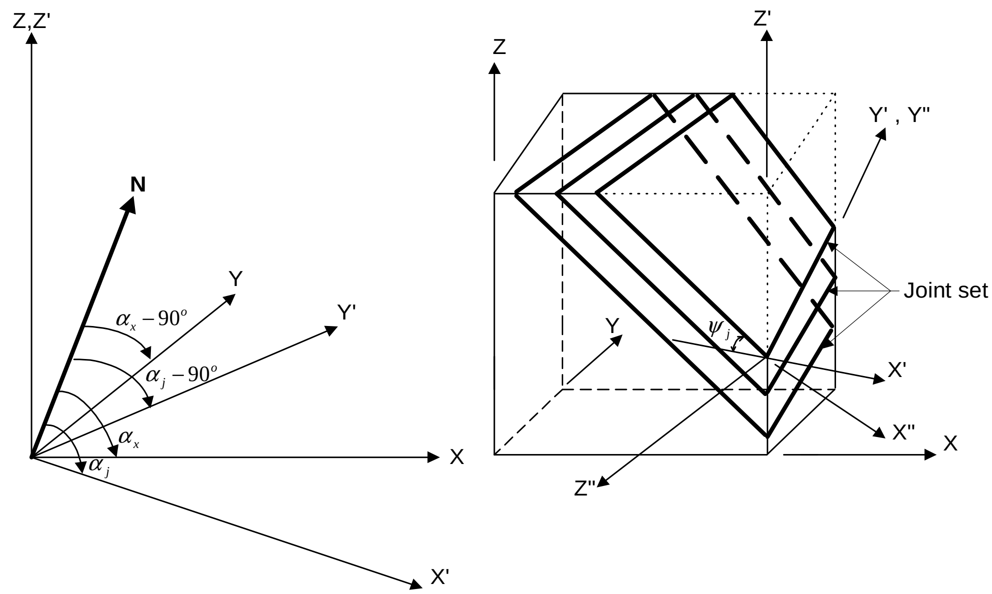

Fig. 1 – Orientation of Axes with respect to a joint plane

Rotate the stresses in vector form, $\{\sigma\}$ with respect to X,Y,Z axes to stresses in vector form, $\{\sigma'\}$ with respect to X′,Y′,Z′ axes as (Malvern, 1969),

$$\{\sigma'\} = \left[T_j{}' \right] \{\sigma\} \tag{5}$$

where,

$$\{\sigma'\} = \left\{ \sigma'_x , \sigma'_y , \sigma'_z , \tau'_{xy} , \tau'_{yz} , \tau'_{zx} \right\}^T \tag{6}$$

$$\{\sigma\} = \left\{ \sigma_x ,\ \sigma_y ,\ \sigma_z ,\ \tau_{xy} ,\ \tau_{yz} ,\ \tau_{zx} \right\}^T \tag{7}$$

and [T_j'] is the first transformation matrix defined in Eq. 3.

The following direction cosines define the rotation between the X′,Y′,Z′ axes and X″,Y″, Z″ axes (Fig. 1b):

$$\begin{aligned} l_1 &= -\cos\psi_j , & m_1 &= 0 , & n_1 &= +\sin\psi_j \\ l_2 &= 0 , & m_2 &= 1 , & n_2 &= 0 \\ l_3 &= -\sin\psi_j , & m_3 &= 0 , & n_3 &= -\cos\psi_j \end{aligned} \tag{8}$$

Based on the above direction cosines, the second transformation matrix, [T_j''] can be written as,

$$\left[\, T_j'' \,\right] = \begin{bmatrix} \cos^2\psi_j & 0 & \sin^2\psi_j & 0 & 0 & -\sin 2\psi_j \\ 0 & 1 & 0 & 0 & 0 & 0 \\ \sin^2\psi_j & 0 & \cos^2\psi_j & 0 & 0 & \sin 2\psi_j \\ 0 & 0 & 0 & -\cos\psi_j & \sin\psi_j & 0 \\ 0 & 0 & 0 & -\sin\psi_j & -\cos\psi_j & 0 \\ \frac{1}{2}\sin 2\psi_j & 0 & -\frac{1}{2}\sin 2\psi_j & 0 & 0 & \cos 2\psi_j \end{bmatrix} \tag{9}$$

Now in second stage, rotate the stresses in vector form, { σ' } referred to X′,Y′,Z′ axes to stresses in vector form, { σ'' } in X″,Y″, Z″ axes using the second transformation matrix, [T_j''] given in Eq. 9. Hence,

$$\{\sigma''\} = \left[\, T_j'' \,\right] \{\sigma'\} \tag{10}$$

where, axis Y″ is parallel to Y′ axis or the strike of the joint plane and the axis, X″ is rotated to lie on the joint plane. Thus, the axis, Z″ is normal to the joint plane.

Finally, the stresses on the joint plane in vector form, { σ'' } consisting of one normal stress and two shear stresses, can be obtained by combining Eq. 5 and Eq. 10 as follows:

$$\{\sigma''\} = \left[\, T_j'' \,\right]\left[\, T_j' \,\right] \{\sigma\} \tag{11}$$

Figure 2 shows that $\sigma_{z''z''}$ is the normal stress on the joint plane and $\tau_{z''x''}$ and $\tau_{z''y''}$ are the shear stresses on the joint plane along the axes X″ and Y″ respectively.

2.2 Elastic Constitutive Equations

It has been assumed that the average strain energy in a unit volume of rock mass is approximately half the product of average stresses and average strains within the rock mass (Hill, 1963). It is also assumed that all joint sets do not essentially interact with each other significantly. In other words, average stress on any joint plane is practically independent of the average stresses of other joint planes. This is equivalent to assuming homogenous stress field in a unit cube of a jointed rock mass so that the strain energy will tend to be the upper bound of the true strain energy. The computed elastic strain will therefore be slightly conservative. The error will reduce as the loaded area becomes much larger than the size of the rock blocks.

The average normal strain, $\varepsilon_{z''z''}$ across the layered rock mass is now related to average stresses by the following expression assuming the compressive stress to be positive:

$$\varepsilon_{z''z''} = \left[\frac{1}{E_r}\right]\sigma_{z''z''} - \upsilon_r\left[\frac{1}{E_r}\right]\sigma_{x''x''} - \upsilon_r\left[\frac{1}{E_r}\right]\sigma_{y''y''} + f_j\,\frac{\sigma_{z''z''}}{k_n} - f_j\,\frac{\tan\beta}{k_s}\left|\tau_{z''x''}\right| - f_j\,\frac{\tan\beta}{k_s}\left|\tau_{z''y''}\right| \tag{12}$$

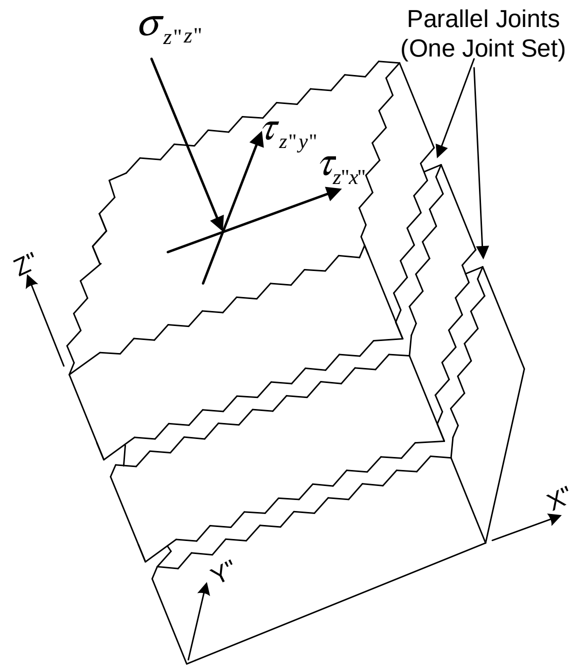

Fig. 2 – Orientation of stresses on a joint plane

where, $\boldsymbol{E_r}$ defines the elastic modulus of the rock material, $\boldsymbol{\upsilon_r}$ is the Poisson's ratio of the rock material, $\boldsymbol{f_j}$ refers to the joint frequency, $\boldsymbol{k_n}$ is the normal stiffness of the joint, $\boldsymbol{k_s}$ is the shear stiffness of the joint, and $\boldsymbol{\beta}$ represents the angle of roughness of the joint.

Assuming that the dilation of joints may be associated with any slip along the rough joints, accordingly the average strain vector contributed by one joint set can be obtained as,

$$\begin{Bmatrix} \varepsilon_{x"x"} \\ \varepsilon_{y"y"} \\ \varepsilon_{z"z"} \\ \gamma_{x"y"} \\ \gamma_{y"z"} \\ \gamma_{z"x"} \end{Bmatrix} = \begin{bmatrix} 0 & 0 & 0 & 0 & 0 & 0 \\ & 0 & 0 & 0 & 0 & 0 \\ & & \dfrac{f_j}{k_n} & 0 & \left[\dfrac{-f_j \ \tan\beta}{k_s} \dfrac{\left|\tau_{y"z"}\right|}{\tau_{y"z"}}\right] & \left[\dfrac{-f_j \ \tan\beta}{k_s} \dfrac{\left|\tau_{z"x"}\right|}{\tau_{z"x"}}\right] \\ & & & 0 & 0 & 0 \\ & & \mathit{Symmetric} & & \dfrac{f_j}{k_s} & 0 \\ & & & & & \dfrac{f_j}{k_s} \end{bmatrix} \begin{Bmatrix} \sigma_{x"x"} \\ \sigma_{y"y"} \\ \sigma_{z"z"} \\ \tau_{x"y"} \\ \tau_{y"z"} \\ \tau_{z"x"} \end{Bmatrix} \quad (13)$$

or $\{\varepsilon''\}_{joint} = [C_j]\{\sigma''\}_{joint}$ (14)

where, **{σ'' }** is the vector of average stresses in a rock mass, **{ε'' }** is the vector of average strains contributed by one joint set, and **[C_j]** is the compliance matrix of the joint set.

With the aid of Eq. 11, stress and strain vectors have been transformed accordingly and, thus, the constitutive equation may be written as,

$$\left[T_j''\right]\left[T_j'\right]\{\varepsilon\}=\left[C_j\right]\left[T_j''\right]\left[T_j'\right]\{\sigma\} \tag{15}$$

so, $$\{\varepsilon\}=\left[T_j'\right]^T\left[T_j''\right]^T\left[C_j\right]\left[T_j''\right]\left[T_j'\right]\{\sigma\} \tag{16}$$

By the addition of average strains contributed by rock material and one joint set in global system, the following relation can be derived:

$$\{\varepsilon\}=\left[\left[C_r\right]+\left[T_j'\right]^T\left[T_j''\right]^T\left[C_j\right]\left[T_j''\right]\left[T_j'\right]\right]\{\sigma\} \tag{17}$$

or $$\{\varepsilon\} = [\,C\,]\ \{\sigma\} \tag{18}$$

where, **[*C*]** is the compliance matrix of a rock mass with single joint set and defined as,

$$[C]=[C_r]+\left[T_j'\right]^T\left[T_j''\right]^T\left[C_j\right]\left[T_j''\right]\left[T_j'\right] \tag{19}$$

and **[C_r]** is the strain-stress matrix (compliance matrix) of the rock material. For an isotropic rock material,

$$[C_r]=\begin{bmatrix} \frac{1}{E_r} & -\frac{\upsilon_r}{E_r} & -\frac{\upsilon_r}{E_r} & 0 & 0 & 0 \\ -\frac{\upsilon_r}{E_r} & \frac{1}{E_r} & -\frac{\upsilon_r}{E_r} & 0 & 0 & 0 \\ -\frac{\upsilon_r}{E_r} & -\frac{\upsilon_r}{E_r} & \frac{1}{E_r} & 0 & 0 & 0 \\ 0 & 0 & 0 & \frac{1}{G_r} & 0 & 0 \\ 0 & 0 & 0 & 0 & \frac{1}{G_r} & 0 \\ 0 & 0 & 0 & 0 & 0 & \frac{1}{G_r} \end{bmatrix} \tag{20}$$

where, G_r is the shear modulus of rock material and given as,

$$G_r = E_r \ / \ 2\,(1 + \upsilon_r) \tag{21}$$

When more than one joint set have been found in the rock mass with different dip direction, α_j and amount of dip, ψ_j , the total strain in the entire jointed rock media is equivalent to the summation of strains contributed by rock material and all the f_j joint sets which intersect the media. Thus, the desired overall strain-stress matrix (compliance matrix) of jointed rock mass may be obtained as,

$$[C] = [C_r] + \sum_{j=1}^{f_j} \left[T_j{}' \right]^T \left[T_j{}'' \right]^T \left[C_j \right] \left[T_j{}'' \right] \left[T_j{}' \right] \tag{22}$$

Inverse of the above matrix is the elasticity matrix, [D] of the jointed rock mass.

For a joint set, $k_n = k_s = 0$ (negligible) have been assumed for $\sigma_{z''z''} > 0$, i.e. it is assumed that the rock mass cannot withstand tensile stresses.

The constitutive relations as derived above, has been incorporated by Samadhiya (1998) in a finite element computer package ASARM. The same package has been used to analyze an underground tunnel to validate the derived constitutive relations.

3. ANALYSIS OF AN UNDERGROUND TUNNEL IN JOINTED ROCKMASS

3.1 Problem Definition

An attempt has been made herein to analyze the problem of a traffic tunnel analyzed earlier by Wittke (1990). The tunnel was excavated at a depth of 250 m below the ground surface. The geometrical details of tunnel are presented in Fig. 3. Two orthogonal joint sets were found in the excavated region dipping at 45^{O} and striking parallel to the tunnel axis. The tunnel was analyzed in 3-D by considering one layer of brick elements. The solution was based on an analysis in which the reduced strength of the two sets of discontinuities was considered. In the present study, anisotropic continuum approach has been applied for 3-D analysis of this tunnel.

The properties of constituents of rock mass are presented in Table 1. Shear stiffness of the joints have been taken as one-tenth of the normal stiffness (Bandis et al., 1981). The rock has been treated as an elastic anisotropic continuum.

The tunnel periphery has been subjected to equivalent loads due to release of in situ stresses. Only part of the height, which may get disturbed due to the excavation process, has been taken into account, while the effect of remaining height has been accounted for by applying a distributed pressure on the top boundary of the mesh. The loads due to in situ stresses have been calculated using the following expressions:

$$\left\{ F_0^e \right\} = \int_V \left[B \right]^T \left\{ \sigma_0 \right\} dV \tag{23}$$

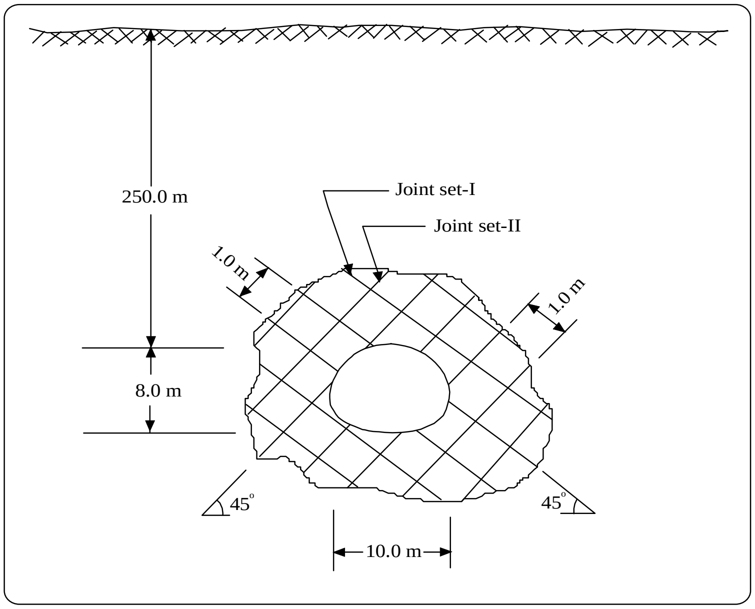

Fig. 3 – Geometrical details of tunnel (Wittke, 1990)

Table 1 - Material Properties (Wittke, 1990)

Material Type	. No.	Property	Value
Intact rock	1.	Young's modulus, E (MPa)	2000
	2.	Poisson's ratio, υ	0.4
	3.	Unit weight, γ (kN/m^3)	25.0
Joint sets	4.	Cohesion, c (MPa)	0.1
	5.	Angle of friction, φ (Deg.)	30
	6.	Normal stiffness, k_n (MPa/m)	3300
	7.	Shear stiffness, k_s (MPa/m)	330
	8.	Spacing of joint, S_j (m)	1.0

where, $\{\sigma_0\} = \{\sigma_{x0}, \sigma_{y0}, \sigma_{z0}\}^T = \{K_x\,\gamma\,z,\, K_y\,\gamma\,z,\, \gamma z\}^T$ (24)

in which $\boldsymbol{K_x}$ and $\boldsymbol{K_y}$ are the coefficients of the lateral earth pressure in X and Y directions respectively, $\boldsymbol{\gamma}$ is the unit weight of rock mass, and z is the depth of Gauss point below ground surface.

In addition, uniformly distributed load of 5.5 MPa acting in the downward direction has been applied on the top surface of the domain. The symmetry of geometry and the loading conditions has been considered. Figure 4 shows the finite element mesh having width, height and length of 36 m, 68 m and 25 m respectively. The mesh comprises of 300, 3-D parabolic brick elements and 1714 nodes.

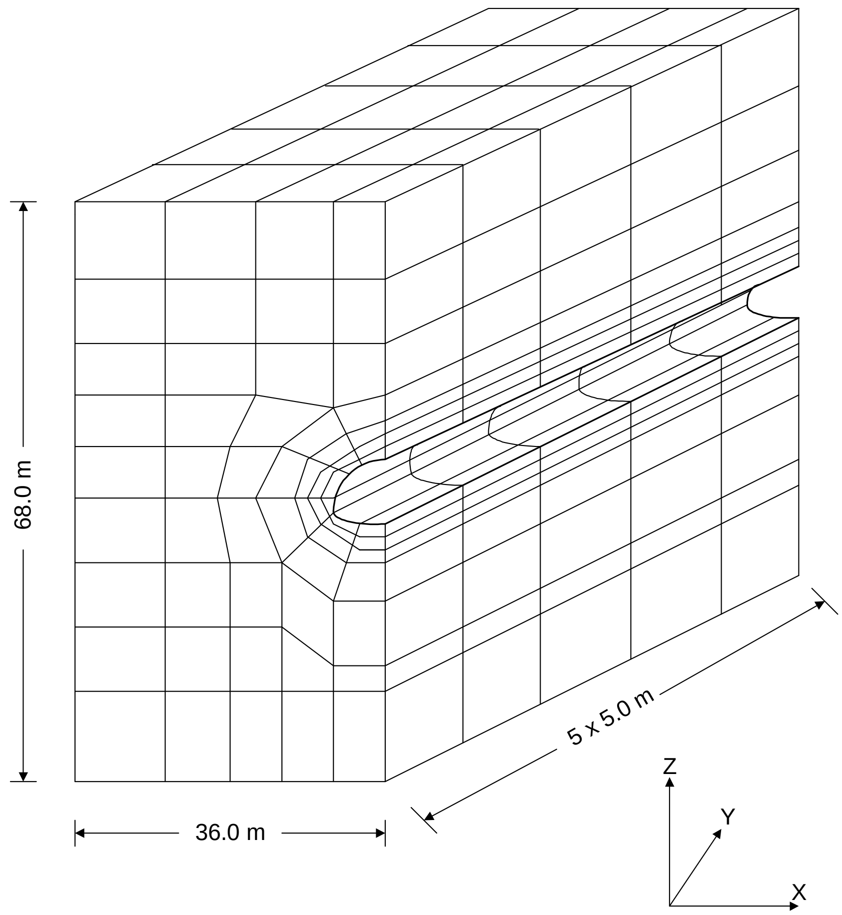

Fig. 4 – 3D Finite element mesh of tunnel

A restrained boundary condition has been imposed in the horizontal direction on all lateral faces of the finite element mesh, whereas the bottom face was retrained in the vertical direction.

3.2 Analysis of Results

(a) Deformed Profile

The displacements deformed profile of the finite element mesh is shown in Fig. 5a. It may be noted that the displaced zone reduces with the distance away from the tunnel periphery. Maximum displacements have been found at tunnel periphery in both the directions. The displacement at the roof of tunnel is 31mm downward whereas it is about 18.5mm upward at the floor of tunnel. At the middle of the sidewall, the vertical and horizontal displacements are 9mm and 8mm respectively directed towards the excavation.

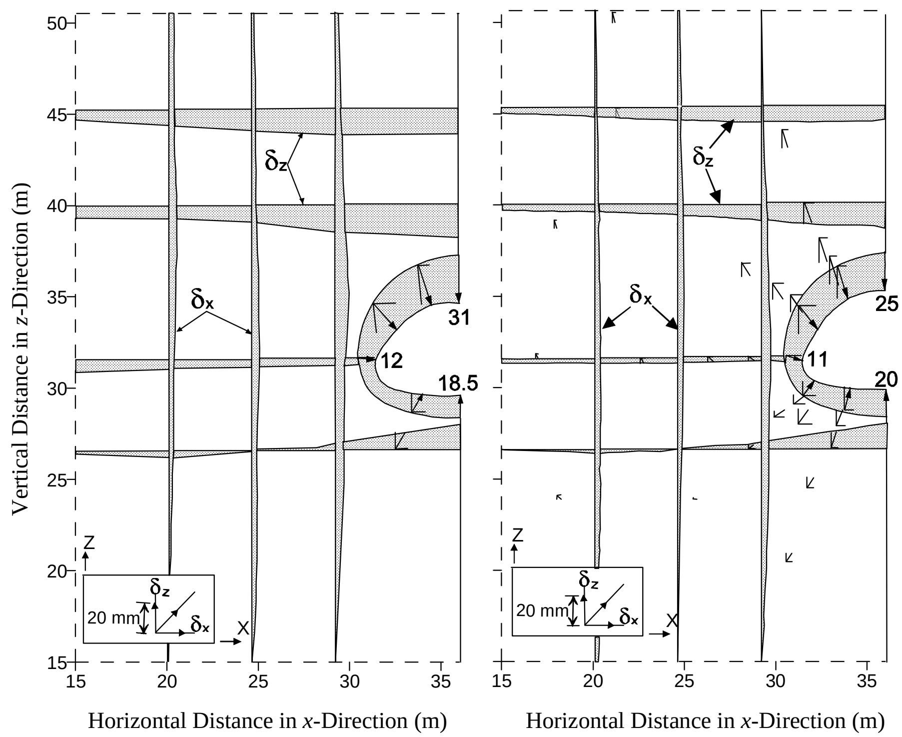

(a) Present Study **(b) After Wittke (1990)**

Fig. 5 – Deformation (mm) profile around an underground opening

The deformed profile obtained by Wittke (1990) is presented in Fig. 5b. It can be observed that displacements obtained in the present study are slightly higher than those obtained by Wittke (1990) in the upper part of tunnel. The opposite is true for the lower part of tunnel. Nevertheless, the deflected shapes remain the same. The differences in deformations may be due to different approaches adopted in arriving at these displacements. Another reason for such a difference may be the difference in some characteristics of joint sets adopted like stiffnesses of joints. These stiffnesses have a pronounced effect on the behavior of rock masses.

From the above interpretation, it may be concluded that anisotropic continuum approach may be effectively used to simulate the anisotropic rock masses. The only limitation of this approach is that displacements along the individual joints can not be obtained.

(b) Deformation Contours

Figure 6a shows the contours of vertical displacements around the tunnel. Larger displacements have been found concentrated near the crown of the tunnel. Comparison with the solution, given by Wittke (1990) in Fig. 6b, reveals a close correspondence and thus further proves that anisotropic continuum approach can be used to analyze structures in anisotropic rock masses.

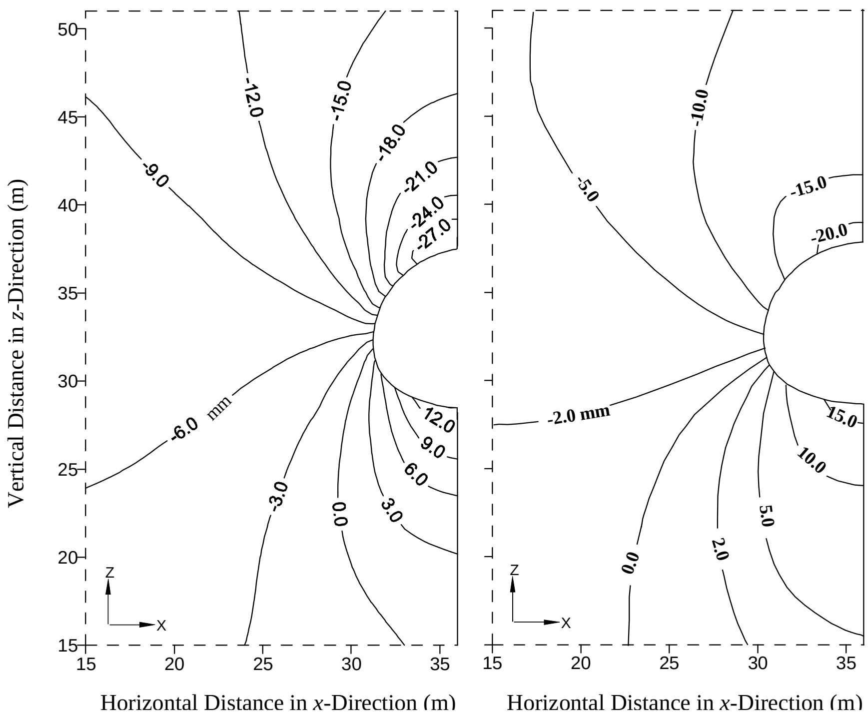

(a) Present Study **(b) After Wittke (1990)**

Fig. 6 – Vertical displacement (mm) contours around an underground opening

(c) Stress Contours

The contours of induced vertical stresses resulting from the excavation of tunnel in anisotropic rock mass are plotted in Fig. 7a. Higher induced compressive stresses of magnitude 6.5 MPa have been recorded in the sidewall of the tunnel. These decrease with distance away from the tunnel wall and reach a value of about 0.5 MPa at about 15 m from the sidewall. At crown, the stresses become tensile with a magnitude of 5.0 MPa.

Similar results were obtained by Wittke (1990) which are presented in Fig. 7b. A very good agreement has been found from both the studies.

(d) Stress Distribution

Re-distribution of stresses at crown and the sidewall of tunnel are presented in Fig. 8a. The stress decreases away from the tunnel periphery and reaches a constant value of about 6.75 MPa at about 10 m from the tunnel wall. At the periphery of tunnel, radial stress has been found to be zero followed by an increasing trend and then a constant value of 4.4 MPa at a distance of about 10 m from the tunnel wall.

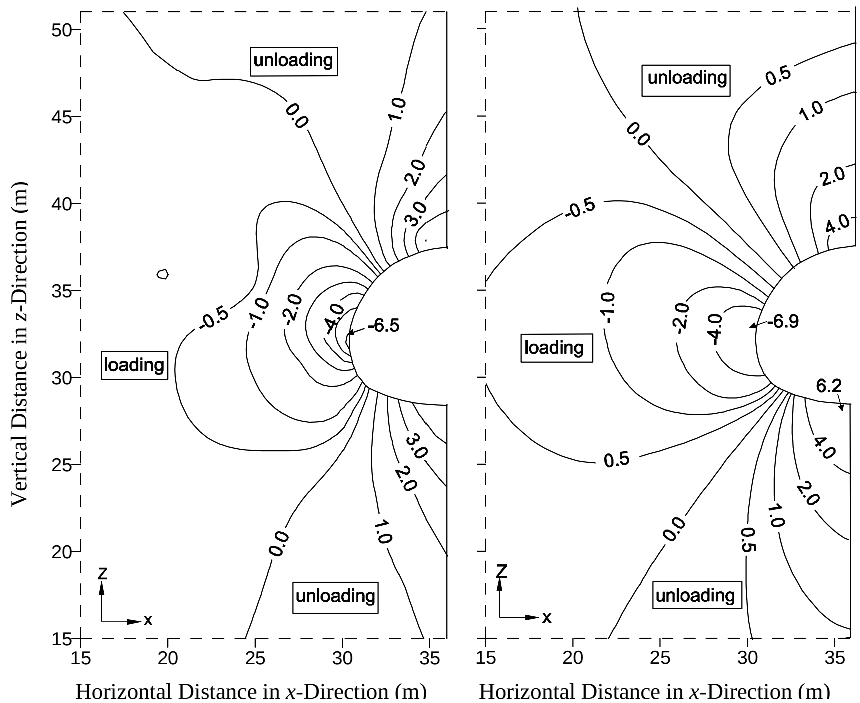

(a) Present Study **(b) After Wittke (1990)**

Fig. 7 – Contours of induced vertical stress (MPa) around an underground opening

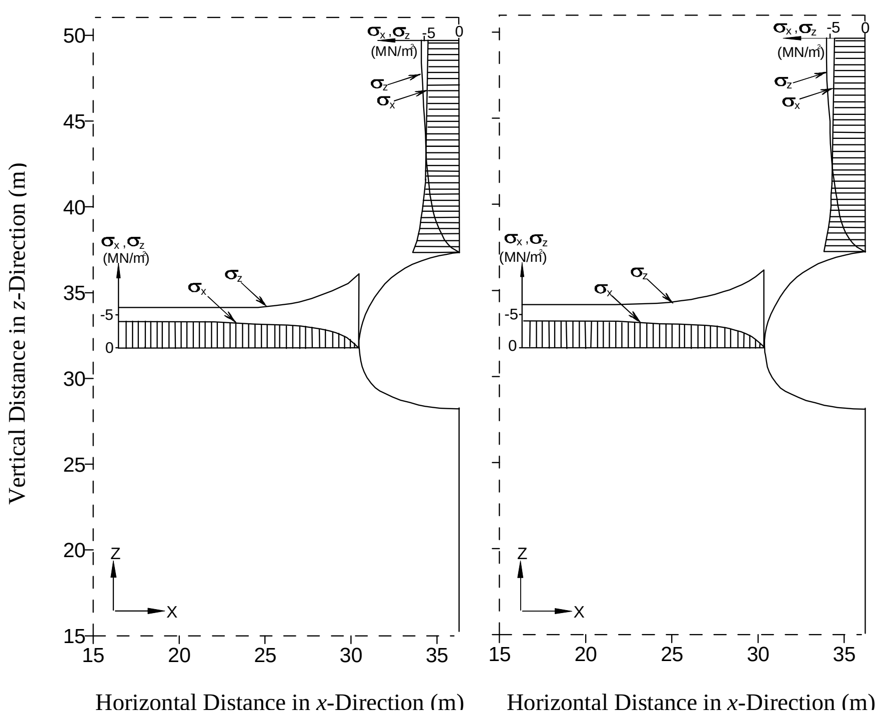

(a) Present Study **(b) After Wittke (1990)**

Fig. 8 – Stress (MPa) distribution at crown and side of underground opening

At the crown, opposite behavior has been found, i.e. maximum radial stress, σ_x, at the periphery of tunnel and then decrease up to a constant value of 4.7 MPa at a distance of about 10 m from crown. The tangential stress, σ_z, is zero at crown and then increases to a value of 5.6 MPa at 10 m from crown. The radial and tangential stresses are in close agreement with those of Wittke (1990), as presented in Fig. 8b

(e) Principal Stress Contours

To illustrate the redistribution of stresses around an opening as a result of excavation of tunnel in the rock mass, the resulting principal stress distribution has been presented in Fig. 9a alongwith the orientation of principal planes. It is clear from this plot that principal stresses are redistributed in magnitude and direction, especially in the vicinity of the excavated tunnel. Insignificant effect has been found of excavation on stress redistribution beyond a distance of 10 m from the tunnel wall. The results are compatible with those by Wittke (1990) as shown in Fig. 9b.

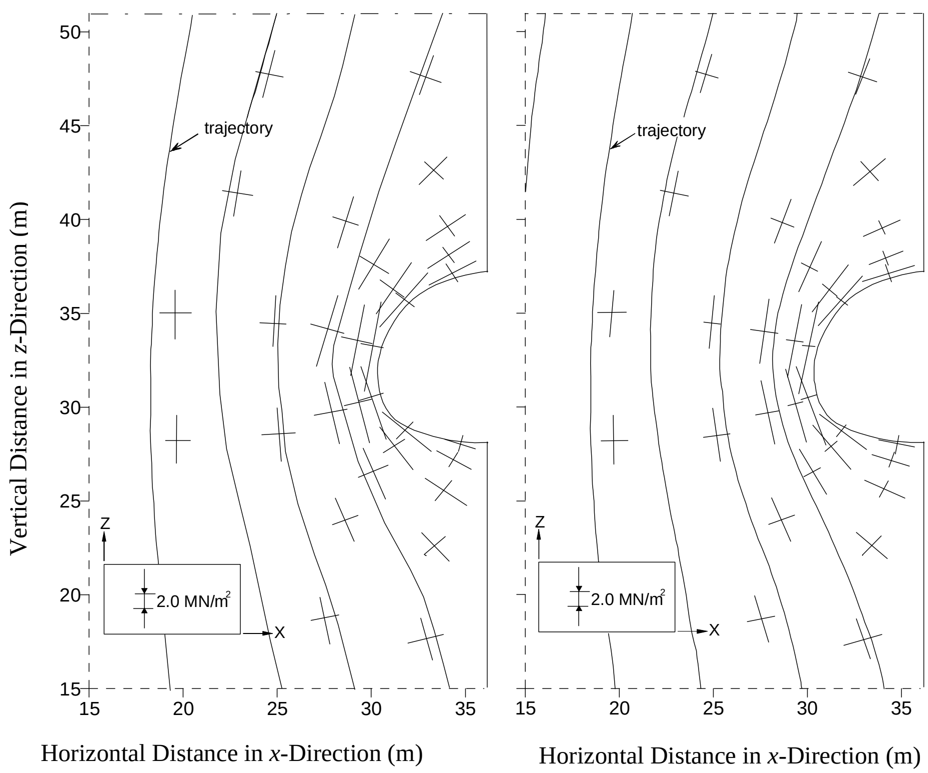

(a) Present Study **(b) After Wittke (1990)**

Fig. 9 – Distribution of principal stresses (MPa) around an underground opening

4. CONCLUSION

Presence of mechanical defects, like joints etc., renders the rock mass to be anisotropic. The joints may occur in the form of regular joint sets, each joint set being characterized by its own dip, dip direction or strike. Mechanical behavior of rock mass is also influenced by the frequency of joints and the number of joint sets. The joints may be dilatant in nature depending upon whether the joint surfaces are rough or smooth. The joints may have in-fillings or gouge material present. Constitutive relationships of the rock mass should therefore reflect the influence of all these parameters so as to obtain a realistic picture of deformations, strains and stresses developed due to different loadings.

An attempt has been made in this paper to present the constitutive relationships for such anisotropic rock masses so that these could be included in the finite element analysis of large tunnels or caverns. As such a very exhaustive and a comprehensive finite element package ASARM has been developed for analyzing underground excavations involving 3-D geometry. A tunnel excavated in an isotropic rock mass has been investigated in detail. The fact that results of the present study corroborate with the results of the earlier investigator (Wittke, 1990) justify the applicability and utility of the constitutive relations.

References

Alehossein, H. and Carter, J. P. (1990). "On the Implicit and Explicit Inclusion of Joint in the Analysis of Rock Masses", *Int. Conf. on Mech. of Jointed and Faulted Rock*, Vienna (Austria), pp. 487-494.

Amadei, B. (1996). "Importance of Anisotropy When Estimating and Measuring In situ Stresses in Rock", *Int. J. Rock Mech. Min. Sci. & Geomech. Abstr*., Vol. 33, No. 3, pp. 293-325.

Amadei, B. and Goodman, R. E. (1981). "A 3D Constitutive Relation for Fractured Rock Masses", *Int. Sym. on the Mechanical Behavior of Structured Media*, Ottawa (Canada), Part B, pp. 249-268.

Bandis, S. C., Lumsden, A. C. and Barton, N. R. (1981). "Experimental Studies of Scale Effects on the Shear Behaviour of Rock Joints", *Int. J. Rock Mech. Min. Sci. & Geomech. Abst*r., Vol. 18, No. 1, pp. -21.

Cai, M. and Horii, H. (1993). "A Constitutive Model and FEM Analysis of Jointed Rock Masses", *Int. J. Rock Mech. Min. Sci. & Geomech. Abstr*., Vol. 30, No. 4, pp. 351-359.

Duncan, J. M. and Goodman, R. E. (1968). "Finite Element Analysis for Slope in Jointed Rock", *Contract Report S-68-3, US Army Waterways Experimentation Station*, Corps. of Engineers, Vicksburg, Mississipi (US).

Fossum, A. F. (1985). "Effective Elastic Properties for a Randomly Jointed Rock Mass", *Int. J. Rock Mech. Min. Sci. & Geomech. Abstr.*, Vol. 22, No. 6, pp. 467-470.

Gerrard, C. M. (1982). "Joint Compliances as a Basis for Rock Mass Properties and the Design of Supports", *Int. J. Rock Mech. Min. Sci. & Geomech. Abstr*., Vol. 19, No. 6, pp. 285-305.

Hill, R. (1963). "Elastic Properties of Reinforced Solids: Some Theoretical Principles", *J. Mech. Phys. Solids*, Vol. 11, pp. 357-372.

Indraratna, B. (1990). "Laboratory Simulation of Joints and their Influence on Rock Mass Behaviour", *Int. Symp. on Rock Joints, Loen (Norway), ISRM*, pp. 235-242.

Ku, C. Y., Lin, J. –S. and Chen, J. –C. (2004), “Modelling of Jointed Rock Masses Using a Combined Equivalent Continuum and Discrete Approach”, *Int. J. Rock Mech. & Min. Sci.*, Vol. 41, No. 3, Paper 2A-15.

Malvern, L. E. (1969). “Introduction to the Mechanics of a Continuous Medium”, Prentice Hall Inc., New Jersey (US).

Pande, G. N. (1993). “Constitutive Models for Intact Rock, Rock Joints and Jointed Rock Masses”, *Comprehensive Rock Engineering (Ed. Hudson J. A.)*, 1st Edition, Pergamon Press, London, Vol. 1, Chap.17, pp. 427-441.

Prat, P. C., Sánchez, F. and Gens, A. (1997). “Equivalent Continuum Anisotropic Microplane Model for Rock: Theory and Applications to Finite Element Analysis”, *6th Int. Symp. on Numerical Methods in Geomech.*, Montreal (Canada), Vol. VI, pp. 159-164.

Rosso, R. S. (1976). “A Comparison of Joint Stiffness Measurments in Direct Shear, Triaxial Compression and In Situ”, *Int. J. Rock Mech. Min. Sci. & Geomech. Abstr*., Vol. 13, No. 6, pp. 167-172.

Samadhiya, N. K. (1998). “Influence of Anisotropy and Shear Zones on Stability of Caverns”, *Ph.D. Thesis*, Dept. of Civil Engng., Univ. of Roorkee, Roorkee (India),p.334.

Singh, B. (1973). “Continuum Characterization of Jointed Rock Masses: Part I- The Constitutive Equations”, *Int. J. Rock Mech. Min. Sci. & Geomech. Abstr*., Vol. 10, No. 4, pp. 311-336.

Sitharam, T. G. and Latha, G. M. (2002). “Simulation of Excavations in Jointed Rock Masses Using a Practical Equivalent Continuum Approach”, *Int. J. Rock Mech. & Min. Sci.*, Vol. 39, No. 4, pp. 517-525.

Wang, B. and Garga, V. K. (1993). “A Numerical Method for Modelling Large Displacements of Jointed Rocks: 1. Fundamentals”, *Candian Geotech. J.*, Vol. 30, No. 1, pp. 96-108.

Wittke, W. (1990). “Rock Mechanics – Theory and Applications with Case Histories”, Springer-Verlag, Berlin (Germany), p. 1075.

Yamabe, T., Oda, M., Ishizuka, Y., Kumasaka, H. and Tado, H. (1990). “Continuum Modelling of Rock Joints and its Application to Three Dimensional Excavation Analysis”, *Int. Symp. on Rock Joints, Loen (Norway), ISRM*, pp. 775-780.